Surname *et al. Vessel Plus* Year;Volume:Number
DOI: 10.20517/2574-1209.xxxx.xx

Vessel Plus

Open Access

Check for updates

Review

Review of CT perfusion and current applications in posterior circulation stroke

Leon S. Edwards[1,2,3], Cecilia Cappelen-Smith[1,2,3], Dennis Cordato[1,2,3], Andrew Bivard[4], Leonid Churilov[4], Mark W. Parsons[1,2,3]

[1]Department of Neurology and Neurophysiology, Liverpool Hospital, Sydney, NSW, Australia.

[2]South Western Sydney Clinical School, University of New South Wales, Sydney, NSW, Australia.

[3]Ingham Institute for Applied Medical Research, Sydney, NSW, Australia.

[4]Melbourne Brain Centre at the Royal Melbourne Hospital, University of Melbourne, Parkville, Australia.

Correspondence to: Prof. Mark W. Parsons, Department of Neurology and Neurophysiology, Liverpool Hospital, Sydney, NSW, Australia E-mail: Mark.Parsons@unsw.edu.au

How to cite this article: Edwards L, Cappelen-Smith C, Cordato D, Bivard A, Churilov L, Parsons M. Review of CT perfusion and applications in posterior circulation stroke. *Vessel Plus* 2021;5:[Accept].http://dx.doi.org/10.20517/2574-1209.2021.18

Received: 1 Feb 2021 **Revised:** 5 Apr 2021 **Accepted:** 20 Apr 2021 **First online:** 31 May 2021

Abstract

Acute ischemic stroke is a leading cause of death and disability. Treatment efficacy is highly time-dependent. Approximately 20% of acute ischaemic stroke occurs in the posterior circulation. Clinical presentation of posterior circulation stroke is subtle. Diagnosis is often delayed and frequently missed. CT perfusion has improved diagnostic accuracy and been integral to guiding acute therapy in patients with anterior circulation stroke. There are limited studies assessing the role of CT perfusion in posterior circulation stroke. This review provides a reference for interpretation of CT perfusion and summarises current evidence relating to applications in acute posterior circulation stroke.

Keywords: CT perfusion, posterior circulation, acute ischaemic stroke

INTRODUCTION

Stroke is globally one of the leading causes of death and disability. Acute treatment for ischaemic stroke is highly effective but partly time-dependent. Treatment depends upon expedient clinical appraisal of medical imaging. Current guidelines use a specific time window from stroke onset to determine eligibility for reperfusion therapy [1][2]. Due to this limited time frame, only a minority of potentially eligible strokes receive acute therapy[3]. Early studies established the role of thrombolysis and endovascular thrombectomy (EVT) within 4.5 h and 6 h from symptom onset, respectively, of an eligible ischaemic stroke. More recent trials have used advanced imaging to demonstrate a benefit of these treatments over an extended time window [3][4][5][6][7]. These studies have expanded the number of patients eligible for acute reperfusion therapies.

Multimodal imaging including CT perfusion (CTP) is recommended by most international guidelines as part of the imaging work up for acute stroke. CT perfusion (CTP) follows the temporal course of an IV bolus of iodinated contrast through the brain parenchyma to calculate multiple parameters. It has allowed clinicians to select patients for therapy based on both time and tissue based characteristics. As such, this modality has underpinned patient selection to trials demonstrating a benefit of acute therapy in the extended time window.

Approximately 20% of strokes occur in the posterior circulation [8][9]. Compared to anterior circulation stroke (ACS), posterior circulation acute ischaemic strokes (PCS) are misdiagnosed three times more frequently [10][11]. PCS frequently present with non-specific symptoms including headache, dizziness and gait disturbance, making the diagnosis difficult on clinical grounds alone [11]. Studies have reported that up to 90% of PCS do not meet the criteria for TIA at first medical contact [12]. This often leads to a delayed or inaccurate diagnosis.

To date, there have been few studies exploring the role of CTP in PCS. Given the limited evidence and technical challenges[13] of performing CTP for PCS, uptake has been limited. Advances in image acquisition, scanner technology and software have overcome many of these barriers. Recent studies of CTP for PCS have demonstrated promising utility including improved diagnostic accuracy[14] and prediction of functional outcomes[15][16].

This review aims to:

1. Provide an overview of the technical aspects involved in CTP acquisition and post processing;

2. Define common CTP parameters reported by existing software;

3. Explore the evidence regarding current ischaemic core and penumbra thresholds;

4. Discuss common technical pitfalls impacting CTP parameters.

5. Summarise existing evidence relating to CTP in PCS including specific technical challenges and current applications.

Overview of CTP

Acquisition of CTP

CTP protocol varies by institution and scanner. Brain coverage is dependent on the number and width of CT detectors. Ideally there should be at least 80 mm of axial coverage [17]. However, to fully capture the posterior fossa and supratentorial brain, whole brain coverage (>100 mm) is ideal. After administration of iodinated contrast, a four dimensional sequence of scans are acquired over a designated period of time. Ideally, to avoid bolus truncation, images should be captured over a minimum of 60 seconds [18][19]. The acquired source images effectively track the course of contrast agent through the brain vasculature and tissue.

Post processing of CTP

The four-dimensional source images are converted into a range of perfusion maps which represent different haemodynamic parameters. Maps are generated via deconvolutional algorithms based on the arterial input function and passage of contrast through each voxel. Common outputs from CTP include mean transit time (MTT), cerebral blood flow (CBF), and cerebral blood volume (CBV). Maps of contrast transit such as Tmax or Delay Time are also produced, depending on software. These parameters are further processed to provide maps that estimate the volume of tissue that is irreversibly damaged, or infarcted (ischemic core), and ischemic tissue at risk of future infarction without reperfusion (penumbra).

Several software packages exist for determination of these parametric maps. Calculation of these maps is vendor-specific with no standardised method for transformation of the raw data. Different mathematical techniques underpin the output represented by these maps[20]. Studies have shown significant differences in perfusion

parameters derived from identical source data depending on software package [21] and post processing method used [20] (Figure 1A-B and Figure 2A-B).

Parameters

There are several considerations when interpreting perfusion maps. The normal ranges for perfusion parameters vary by anatomical location[22], age and neurological state[23]. Cerebral haemodynamics are autoregulated via complex metabolic mechanisms including blood pressure, arterial partial pressure of carbon dioxide and pH.

Perfusion parameters represent the temporal characteristics of contrast as it travels from the arterial system through the brain parenchyma. The two principal determinants of this transit are arterial flow and intrinsic tissue characteristics. Arterial flow is approximated by the arterial input function. Factors that cause delay and dispersion of arterial flow include: reduced cardiac output, arterial stenosis, and injection rate [24]. Tissue perfusion is mathematically deducted via deconvolution using the arterial input function to account for arterial flow.

Mean transit time (MTT)

MTT represents the mean time for blood to pass through a voxel. It is correlated with mean arterial pressure and cerebral perfusion pressure and is measured in seconds [25].

Cerebral blood volume (CBV)

CBV is the fraction of blood vessels in a single voxel. It is measured in millilitres/100g [26].

Cerebral blood flow (CBF)

CBF is the flow rate of blood through a single voxel in a given time. It is mathematically related to CBV and MTT via the central volume principle which states CBF = CBV/MTT [26]. CBF is measured in millilitres/100 g/min.

Time-density relationship measures (Time to peak [TTP], Time to drain [TTD], Tmax and Delay Time [DT]). These parameters provide a visual interpretation of the time density curve. They reflect the time taken from the start of the scan to the maximum

recordable intensity of the contrast medium in brain tissue. Although related, different mathematical methods underlie the calculation of these perfusion parameters [27][22]. An in-depth discussion of these parameters lies outside the scope of this review. Time-density relationship parameters are measured in seconds.

Time to peak (TTP)

TTP is a simple yet robust measure of blood flow[28][29]. This parameter represents the time from contrast injection to the maximum tissue enhancement value. Importantly, this parameter does not incorporate deconvolution, as such is sensitive to delay and dispersion of contrast bolus. Failure to correct for delay and dispersion may lead to overestimation of core and underestimation of penumbral volumes [30][31].

Tmax

Tmax is also known as the time of peak of the deconvolved tissue residual function [32]. This parameter represents the time from arterial peak to the peak of the tissue concentration curve, after a deconvolution algorithm has been applied. This measure is sensitive to delay in arrival of the contrast bolus. Indeed, in normal tissue Tmax should equal zero.

Delay time (DT)

Delay time is somewhat similar to Tmax, but has been corrected for both delay and dispersion of the contrast bolus. The problem with not correcting for both delay and dispersion is that the contrast bolus is dispersed (via collateral pathways) by the time it reaches the ischemic region. This means that the "real" tissue arterial concentration/time curve is "shorter and fatter" than in the proximal arteries [33][34]. Failure to correct for this leads to overestimation of the true contrast transit and inaccurate estimation of "true" perfusion lesion volume [30].

Time to drain (TTD)

This is a deconvolution-based parameter which measures the time taken for contrast medium washout. It is based on the time from arterial enhancement to tissue enhancement (Time to start) and MTT [35]. It is sensitive to multiple haemodynamic disturbance not necessarily captured by Tmax, delay time or Time to peak

CTP thresholds

Core

Accurate measurement of ischemic core has been fundamental for patient selection in clinical trials of acute reperfusion therapy. Large core volume is a predictor of poor outcome [36] and complication [37] following acute reperfusion therapies. Conversely, overestimation of core may unnecessarily preclude patients from receiving beneficial treatment [30].

Both CBV [22][38] and CBF have been validated to estimate ischaemic core volume. While early studies and guidelines utilised CBV, more recently, CBF thresholds have become the standard for defining core estimates. Multiple CBF thresholds have been correlated with final infarct size [39][40][20]. A CBF threshold of <30% has been most extensively validated, but only in the anterior circulation [32][34][17] (Figure 1C and Figure 2C).

It is important to note that studies defining the optimal CTP thresholds for core have been typically based on final infarct size on follow up MRI. CTP measures the transit of contrast through brain tissue rather than cellular injury (which Diffusion-weighted imaging/DWI lesions reflect) [41]. As such, these thresholds do not represent real infarct tissue but are projected representations of tissue fate. Several factors have been shown to result in CTP overestimates of core estimates including: a shorter time from stroke onset to imaging [42] and rapid reperfusion [43]. Conversely, in conditions where blood flow and volume are restored to infarcted brain tissue, such as late recanalisation or improved collateral flow, CTP may appear normal, despite a relatively large infarct. Wherever possible, clinicians should validate CTP core representations by cross referencing these maps with the “raw” CTP perfusion maps as well as non-contrast CT (NCCT) images to corroborate actual infarct volume.

Penumbra

In stroke, penumbra represents the hypoxic cerebral tissue at risk of irreversible damage which is potentially salvageable with restoration of blood flow. Penumbral volume is equal to the area of critically hypoperfused brain tissue minus the ischaemic

core. Early imaging studies exploring penumbra were based on final infarct volume of hemispheric strokes with persistent large artery occlusion [38][41][44].

Several parameters have been validated as successfully approximating penumbra including MTT, TTD, Tmax and DT. Of these markers, DT and Tmax have been shown to be the most accurate markers of penumbra [20]. Delayed time greater than 3 seconds [17] and Tmax greater than 6 seconds [32] have become the generally accepted thresholds for quantifying penumbra. Again, however, these thresholds are not validated in the posterior circulation.

Technical factors

Vessel selection

Arterial and venous selection is automated in several perfusion software packages [45][20]. The selection of these landmarks underpins the arterial input function (AIF) and venous output function (VOF) used in the deconvolution algorithms that estimate perfusion (Figure 3). Inaccurate vessel selection negatively impacts the integrity of the perfusion estimates [46][47].

Patient positioning and movement

Software packages use the contralateral hemisphere as a reference to detect asymmetries in contrast flow indicative of core or penumbra [26]. Head tilt distorts the axial comparison of anatomical structures leading to spurious results. Patient movement can be corrected to a degree via the software vendors' automated motion adjustment [48][49]. However, significant patient motion can result in distorted perfusion estimates and, at times, artefactual perfusion "lesions".

Radiation exposure

A standard CTP acquires at 80 kilovoltage peak (kVp) and 100 milliamperes-second (mAs). Utilising optimised protocols [50] and multidetector scanners [51], the radiation dose is approximately 2 mSv, which is similar to a single head CT [52] or

approximately 1 year of natural background radiation. Additional imaging must always balance the improved diagnostic information versus the risk of extra radiation.

Z-axis coverage

The number of data channels used in the craniocaudal plane (z-axis) and effective detector thickness influence the z-axis coverage of a CT scanner [53]. For example, a 64 row detector scanner with a detector thickness of 0.5mm has 32 mm of simultaneous z-axis coverage. Detector configuration and z-axis coverage vary considerably by manufacturer [54]. In recent years, there has been growing availability of 320-detector row scanners able to acquire up to 160mm of brain in a single acquisition [17].

CTP in the Posterior Circulation

Studies have routinely demonstrated the utility of CTP perfusion in ACS for both diagnosis [55] and patient selection for acute therapies [3][4][5][6][7]. In contrast, there have been few studies examining the role of CTP in the posterior circulation (PCS). To date, studies have been limited to small retrospective populations [56][57] and case reports [58]. We summarise the existing evidence.

Specific Challenges

Until recently, restricted axial slice coverage has limited the application of CTP to PCS. Older 16 and 64 detector row scanners have a limited scan range of 20-40mm in the axial plane. As such, scans have been generally focused on capturing regions supplied by the anterior circulation with limited coverage of posterior circulation structures[59]. This has resulted in missed infarcts and underestimates of the ischaemic core and penumbra[60]. Beam hardening artifact and radiation dose have also been considerations affecting quality and safety of PCS CTP [13]. Ultimately, these technical considerations have contributed to limited uptake. A substudy of the Basilar artery international co-operation study (BASICS) registry, the largest prospective dataset of PCS due to acute basilar artery occlusion, demonstrated that only 4.6% of patients underwent CTP [61]. Advances in both software and hardware have enabled whole brain coverage, thereby overcoming many of these challenges. One such advance includes the “toggling-technique” which expands coverage of limited range scanners by jogging between two location acquiring axial images in a to-and-fro manner [62][63].

Similarly, there is greater availability of multi detector scanners with wide z-axis coverage [17][60] able to image the entire brain in a single acquisition slab.

Applications in posterior circulation stroke

Several studies have demonstrated an improvement in diagnostic accuracy when CTP is combined with NCCT and CT angiography source images (CTA-SI) compared to NCCT and CTA-SI alone for the diagnosis of PCS [15][16]. Furthermore, it may hold additional prognostic information to guide acute treatment decisions including reperfusion therapy [64] and surgical intervention [65]. Indeed, a study by Becks et al. reported that the incremental detection benefit of CTP added to NCCT and CTA-SI was only seen in PCS and distal stroke[16]. Studies of early generation scanners with limited scan range demonstrated lower rates of perfusion abnormality in PCS compared to ACS [59]. In contrast, more recent studies of newer whole brain CTP have demonstrated no significant difference in the detection of PCS compared to ACS with a sensitivity of 41.4%-81.4% and specificity of 93.4%-96% [56][57].

MRI is considered the gold standard for diagnosis of PCS [66]. Its utility in the emergency setting of acute stroke is restricted by acquisition time, limited 24/7 availability and inability to be performed in patients with metal foreign bodies such as pacemakers. CTP does not face these challenges. Additionally, MRI within 24-48h of symptoms has been reported to miss as many of 12%-20% of PCS [66][67][68][69]. Choi et al. demonstrated in a cohort of PCS presenting with vertigo or dizziness and DWI MRI confirmed stroke, that 4% had a negative early DWI MRI when performed within 48h. However, when perfusion imaging (CT or MRI) was added to clinical assessment (Head impulse, nystagmus, test of skew, plus acute hearing loss detected by finger rubbing), 100% of these early strokes missed on MRI were detected [70].

PCS due to acute basilar artery occlusion is associated with a high rate of death and disability[71]. The optimal treatment pathway for this condition has not been established [71][72]. Even in the era of endovascular thrombectomy, the rate of good functional outcome remains at ~ 30% [73]. The Posterior circulation Alberta stroke program early CT score (pc-ASPECTS) has been used to predict outcome after vertebrobasilar stroke [74]. Studies have demonstrated improved detection of ischaemic lesions when using CTP compared to CTA-SI alone for assessment of pc-ASPECTS [61][75]. Furthermore, CTP-based assessment demonstrated substantially better

inter-rater agreement and was predictive of functional outcome [75]. This ability to accurately identify lesions and predict outcome may help to guide therapy.

PCS perfusion abnormalities vary considerably depending on the site of vascular occlusion (Figure 4A-B). The size and distribution of the perfusion lesion are influenced by the involvement of different posterior circulation vessels including the basilar, vertebral, cerebellar or posterior cerebral arteries. It has been well established that CTP is less sensitive in detection of small volume infarcts than DWI [76]. Multiple studies have confirmed the factors associated with reduced sensitivity of PCS detection include small stroke volume and location outside of the cerebellum [56] or posterior cerebral artery territory [15]. Small brainstem strokes are not well visualised. Despite this lower sensitivity, NCCT alone is even less sensitive in detecting PCS [77]. A study by Ostman et al. demonstrated that compared to non-enhanced CT, CTP improved sensitivity in detecting cerebellar lesions from 12% to 52% [14]. This difference was even more pronounced in cerebellar lesions greater than 5ml with sensitivity increasing from 32% to 91%.

Among the perfusion parameters, MTT [61][57], TTD [56] and TTP [57] have been most frequently reported as sensitive markers of PCS. Similarly, CBV has been shown to be a specific marker of PCS ischaemia [56][57]. To date, there have been no studies characterising the optimal perfusion threshold for ischaemic core and penumbra volume in PCS. Current proprietary automated core and penumbra maps are based on thresholds derived from anterior circulation stroke [17][32][34][38][41][44]. As such, caution should be applied to automated estimates of core and penumbra in PCS until these thresholds are validated. It is prudent for clinicians to inspect the raw perfusion maps as lesions may be apparent at subthreshold levels (Figure 1C and Figure 2C).

Future directions

CTP has been integral to studies of acute therapies over the extended time window [3][4][6][7]. Ma et al. used CTP-based criteria to select patients who benefit from thrombolysis up to 9 h after stroke onset. Further RCTs are underway exploring even later window thrombolysis utilising CTP-based selection criteria [Tenecteplase in Stroke Patients Between 4.5 and 24 h (TIMELESS), NCT03785678 and Extending the time window for Tenecteplase by Effective Reperfusion of peNumbrAL tissue in patients with Large Vessel Occlusion (ETERNAL), NCT04454788]. Unfortunately,

these studies have been limited to patients with acute hemispheric infarction. Given the promising diagnostic applications of CTP for PCS, future trials of acute therapy using CTP based selection may be warranted.

CONCLUSION

CTP performed for suspected PCS facilitates important diagnostic and prognostic information and can be rapidly acquired in the emergency setting. Historically, uptake in suspected PCS has been poor due to technical challenges. With the wider availability of scanners capable of whole brain coverage and strategies to reduce radiation exposure, routine CTP in all patients with suspected acute PCS may be worthwhile. However, at present perfusion thresholds are not validated for PCS, and expert assessment of raw perfusion maps is advised.

DECLARATIONS

Acknowledgments

Anyone who contributed towards the article but does not meet **the criteria** for authorship, including those who provided professional writing services or materials, should be acknowledged. Authors should obtain permission to acknowledge from all those mentioned in the Acknowledgments section. This section is not added if the author does not have anyone to acknowledge.

Authors' contributions

LSE was the principal author of the manuscript

CCS was involved in drafting and revision of the manuscript

DC was involved in drafting and revision of the manuscript

AB was involved in drafting and revision of the manuscript

LC was involved in drafting and revision of the manuscript

MWP was involved in conception, drafting and revision of the manuscript

Availability of data and materials

Not applicable.

Financial support and sponsorship

None.

Conflicts of interest

All authors declared that there are no conflicts of interest.

Ethical approval and consent to participate

Not applicable.

Consent for publication

Not applicable.

REFERENCES

[1] W. J. Powers et al., "Guidelines for the Early Management of Patients With Acute Ischemic Stroke: 2019 Update to the 2018 Guidelines for the Early Management of Acute Ischemic Stroke: A Guideline for Healthcare Professionals From the American Heart Association/American Stroke Association," Stroke, vol. 50, no. 12, pp. e344–e418, Dec. 2019.

[2] National Stroke Foundation (Australia), Clinical Guidelines for Stroke Management 2010. 2010.

[3] A. T. Rai et al., "A population-based incidence of acute large vessel occlusions and thrombectomy eligible patients indicates significant potential for growth of endovascular stroke therapy in the USA," J. Neurointerv. Surg., vol. 9, no. 8, pp. 722–726, Aug. 2017.

[4] H. Ma et al., "Thrombolysis Guided by Perfusion Imaging up to 9 Hours after Onset of Stroke," N. Engl. J. Med., vol. 380, no. 19, pp. 1795–1803, May 2019.

[5] G. Thomalla et al., "MRI-Guided Thrombolysis for Stroke with Unknown Time of Onset," N. Engl. J. Med., vol. 379, no. 7, pp. 611–622, Aug. 2018.

[6] R. G. Nogueira et al., "Thrombectomy 6 to 24 Hours after Stroke with a Mismatch between Deficit and Infarct," N. Engl. J. Med., vol. 378, no. 1, pp. 11–21, Jan. 2018.

[7] G. W. Albers et al., "Thrombectomy for Stroke at 6 to 16 Hours with Selection by Perfusion Imaging," N. Engl. J. Med., vol. 378, no. 8, pp. 708–718, Feb. 2018.

[8] J. Bamford, P. Sandercock, M. Dennis, J. Burn, and C. Warlow, "Classification and natural history of clinically identifiable subtypes of cerebral infarction," Lancet, vol. 337, no. 8756, pp. 1521–1526, Jun. 1991.

[9] U. G. Schulz and U. Fischer, "Posterior circulation cerebrovascular syndromes: diagnosis and management," J. Neurol. Neurosurg. Psychiatry, vol. 88, no. 1, pp. 45–53, Jan. 2017.

[10] A. A. Tarnutzer, S.-H. Lee, K. A. Robinson, Z. Wang, J. A. Edlow, and D. E. Newman-Toker, "ED misdiagnosis of cerebrovascular events in the era of modern neuroimaging: A meta-analysis," Neurology, vol. 88, no. 15, pp. 1468–1477, Apr. 2017.

[11] A. E. Arch, D. C. Weisman, S. Coca, K. V. Nystrom, C. R. Wira 3rd, and J. L. Schindler, "Missed Ischemic Stroke Diagnosis in the Emergency Department by Emergency Medicine and Neurology Services," Stroke, vol. 47, no. 3, pp. 668–673, Mar. 2016.

[12] N. L. M. Paul, M. Simoni, P. M. Rothwell, and Oxford Vascular Study, "Transient isolated brainstem symptoms preceding posterior circulation stroke: a population-based study," Lancet Neurol., vol. 12, no. 1, pp. 65–71, Jan. 2013.

[13] M. Wintermark, N. J. Fischbein, W. S. Smith, N. U. Ko, M. Quist, and W. P. Dillon, "Accuracy of dynamic perfusion CT with deconvolution in detecting acute hemispheric stroke," AJNR Am. J. Neuroradiol., vol. 26, no. 1, pp. 104–112, Jan. 2005.

[14] C Ostman, C Garcia-Esperon, T Lillicrap, S Tomari, E Holliday, C Levi, A Bivard, M Parsons and N Spratt., "Multimodal computed tomography increases the detection of posterior fossa strokes compared to brain non-contrast computed tomography," Front. Neurol., vol. 11, p. 1473, Nov. 2020.

[15] E. J. R. J. van der Hoeven et al., "Additional diagnostic value of computed tomography perfusion for detection of acute ischemic stroke in the posterior circulation," Stroke, vol. 46, no. 4, pp. 1113–1115, Apr. 2015.

[16] M. J. Becks et al., "Brain CT perfusion improves intracranial vessel occlusion detection on CT angiography," Journal of Neuroradiology, vol. 46, no. 2. pp. 124–129, 2019, doi: 10.1016/j.neurad.2018.03.003.

[17] L. Lin, A. Bivard, V. Krishnamurthy, C. R. Levi, and M. W. Parsons, "Whole-Brain CT Perfusion to Quantify Acute Ischemic Penumbra and Core," Radiology, vol. 279, no. 3, pp. 876–887, Jun. 2016.

[18] J. Demeestere, A. Wouters, S. Christensen, R. Lemmens, and M. G. Lansberg, "Review of Perfusion Imaging in Acute Ischemic Stroke: From Time to Tissue," Stroke, vol. 51, no. 3, pp. 1017–1024, Mar. 2020.

[19] S. Christensen and M. G. Lansberg, "CT perfusion in acute stroke: Practical guidance for implementation in clinical practice," J. Cereb. Blood Flow Metab., vol. 39, no. 9, pp. 1664–1668, Sep. 2019.

[20] A. Bivard, C. Levi, N. Spratt, and M. Parsons, "Perfusion CT in acute stroke: a comprehensive analysis of infarct and penumbra," Radiology, vol. 267, no. 2, pp. 543–550, May 2013.

[21] K. Kudo et al., "Differences in CT perfusion maps generated by different commercial software: quantitative analysis by using identical source data of acute stroke patients," Radiology, vol. 254, no. 1, pp. 200–209, Jan. 2010.

[22] C. Chen, A. Bivard, L. Lin, C. R. Levi, N. J. Spratt, and M. W. Parsons, "Thresholds for infarction vary between gray matter and white matter in acute ischemic

447 stroke: A CT perfusion study," Journal of Cerebral Blood Flow & Metabolism, vol. 39,
448 no. 3. pp. 536–546, 2019, doi: 10.1177/0271678x17744453.

449 [23] M. Wintermark, P. Maeder, J. P. Thiran, P. Schnyder, and R. Meuli, "Quantitative
450 assessment of regional cerebral blood flows by perfusion CT studies at low injection
451 rates: a critical review of the underlying theoretical models," Eur. Radiol., vol. 11, no. 7,
452 pp. 1220–1230, 2001.

453 [24] C. Garcia-Esperon et al., "Computed Tomography Perfusion Identifies Patients
454 With Stroke With Impaired Cardiac Function," Stroke, vol. 51, no. 2, pp. 498–503, Feb.
455 2020.

456 [25] P. Schumann, O. Touzani, A. R. Young, R. Morello, J. C. Baron, and E. T.
457 MacKenzie, "Evaluation of the ratio of cerebral blood flow to cerebral blood volume as
458 an index of local cerebral perfusion pressure," Brain, vol. 121 (Pt 7), pp. 1369–1379,
459 Jul. 1998.

460 [26] A. Vagal et al., "Automated CT perfusion imaging for acute ischemic stroke:
461 Pearls and pitfalls for real-world use," Neurology, vol. 93, no. 20, pp. 888–898, Nov.
462 2019.

463 [27] A. Wouters et al., "A Comparison of Relative Time to Peak and Tmax for
464 Mismatch-Based Patient Selection," Front. Neurol., vol. 8, p. 539, Oct. 2017.

465 [28] J. R. Reichenbach et al., "Acute stroke evaluated by time-to-peak mapping during
466 initial and early follow-up perfusion CT studies," AJNR Am. J. Neuroradiol., vol. 20,
467 no. 10, pp. 1842–1850, Nov. 1999.

468 [29] R. Meagher and J. J. S. Shankar, "CT Perfusion in Acute Stroke: 'Black Holes' on
469 Time-to-Peak Image Maps Indicate Unsalvageable Brain," Journal of Neuroimaging,
470 vol. 26, no. 6. pp. 605–611, 2016, doi: 10.1111/jon.12352.

471 [30] L. Lin et al., "Correction for Delay and Dispersion Results in More Accurate
472 Cerebral Blood Flow Ischemic Core Measurement in Acute Stroke," Stroke, vol. 49, no.
473 4, pp. 924–930, Apr. 2018.

474 [31] F. Calamante, D. G. Gadian, and A. Connelly, "Delay and dispersion effects in
475 dynamic susceptibility contrast MRI: simulations using singular value decomposition,"
476 Magn. Reson. Med., vol. 44, no. 3, pp. 466–473, Sep. 2000.

[32] B. C. V. Campbell et al., "Comparison of computed tomography perfusion and magnetic resonance imaging perfusion-diffusion mismatch in ischemic stroke," Stroke, vol. 43, no. 10, pp. 2648–2653, Oct. 2012.

[33] B. C. Campbell and M. W. Parsons, "Imaging selection for acute stroke intervention," Int. J. Stroke, vol. 13, no. 6, pp. 554–567, Aug. 2018.

[34] Y. Yu et al., "Defining Core and Penumbra in Ischemic Stroke: A Voxel- and Volume-Based Analysis of Whole Brain CT Perfusion," Sci. Rep., vol. 6, p. 20932, Feb. 2016.

[35] K. M. Thierfelder et al., "Whole-brain CT perfusion: reliability and reproducibility of volumetric perfusion deficit assessment in patients with acute ischemic stroke," Neuroradiology, vol. 55, no. 7, pp. 827–835, Jul. 2013.

[36] A. J. Yoo, L. A. Verduzco, P. W. Schaefer, J. A. Hirsch, J. D. Rabinov, and R. G. González, "MRI-based selection for intra-arterial stroke therapy: value of pretreatment diffusion-weighted imaging lesion volume in selecting patients with acute stroke who will benefit from early recanalization," Stroke, vol. 40, no. 6, pp. 2046–2054, Jun. 2009.

[37] G. Thomalla et al., "Prediction of malignant middle cerebral artery infarction by magnetic resonance imaging within 6 hours of symptom onset: A prospective multicenter observational study," Ann. Neurol., vol. 68, no. 4, pp. 435–445, Oct. 2010.

[38] M. Wintermark et al., "Perfusion-CT assessment of infarct core and penumbra: receiver operating characteristic curve analysis in 130 patients suspected of acute hemispheric stroke," Stroke, vol. 37, no. 4, pp. 979–985, Apr. 2006.

[39] A. Bivard, N. Spratt, C. Levi, and M. Parsons, "Perfusion computer tomography: imaging and clinical validation in acute ischaemic stroke," Brain, vol. 134, no. Pt 11, pp. 3408–3416, Nov. 2011.

[40] C. W. Cereda et al., "A benchmarking tool to evaluate computer tomography perfusion infarct core predictions against a DWI standard," J. Cereb. Blood Flow Metab., vol. 36, no. 10, pp. 1780–1789, Oct. 2016.

[41] J. Mintorovitch, G. Y. Yang, H. Shimizu, J. Kucharczyk, P. H. Chan, and P. R. Weinstein, "Diffusion-weighted magnetic resonance imaging of acute focal cerebral

ischemia: comparison of signal intensity with changes in brain water and Na+,K(+)-ATPase activity," J. Cereb. Blood Flow Metab., vol. 14, no. 2, pp. 332–336, Mar. 1994.

[42] S. Boned et al., "Admission CT perfusion may overestimate initial infarct core: the ghost infarct core concept," J. Neurointerv. Surg., vol. 9, no. 1, pp. 66–69, Jan. 2017.

[43] C. D. d'Esterre et al., "Time-Dependent Computed Tomographic Perfusion Thresholds for Patients With Acute Ischemic Stroke," Stroke, vol. 46, no. 12, pp. 3390–3397, Dec. 2015.

[44] B. D. Murphy et al., "Identification of Penumbra and Infarct in Acute Ischemic Stroke Using Computed Tomography Perfusion–Derived Blood Flow and Blood Volume Measurements," Stroke, vol. 37, no. 7. pp. 1771–1777, 2006, doi: 10.1161/01.str.0000227243.96808.53.

[45] M. Straka, G. W. Albers, and R. Bammer, "Real-time diffusion-perfusion mismatch analysis in acute stroke," J. Magn. Reson. Imaging, vol. 32, no. 5, pp. 1024–1037, Nov. 2010.

[46] S. M. Kealey, V. A. Loving, D. M. Delong, and J. D. Eastwood, "User-defined vascular input function curves: influence on mean perfusion parameter values and signal-to-noise ratio," Radiology, vol. 231, no. 2, pp. 587–593, May 2004.

[47] I. van der Schaaf, E.-J. Vonken, A. Waaijer, B. Velthuis, M. Quist, and T. van Osch, "Influence of partial volume on venous output and arterial input function," AJNR Am. J. Neuroradiol., vol. 27, no. 1, pp. 46–50, Jan. 2006.

[48] B. C. V. Campbell et al., "Imaging selection in ischemic stroke: feasibility of automated CT-perfusion analysis," Int. J. Stroke, vol. 10, no. 1, pp. 51–54, Jan. 2015.

[49] F. Fahmi et al., "3D movement correction of CT brain perfusion image data of patients with acute ischemic stroke," Neuroradiology, vol. 56, no. 6, pp. 445–452, Jun. 2014.

[50] E. Tong and M. Wintermark, "CTA-enhanced perfusion CT: an original method to perform ultra-low-dose CTA-enhanced perfusion CT," Neuroradiology, vol. 56, no. 11, pp. 955–964, Nov. 2014.

[51] S. Diekmann et al., "Dose exposure of patients undergoing comprehensive stroke imaging by multidetector-row CT: comparison of 320-detector row and 64-detector row CT scanners," AJNR Am. J. Neuroradiol., vol. 31, no. 6, pp. 1003–1009, Jun. 2010.

[52] J. J. Heit and M. Wintermark, "Perfusion Computed Tomography for the Evaluation of Acute Ischemic Stroke: Strengths and Pitfalls," Stroke, vol. 47, no. 4, pp. 1153–1158, Apr. 2016.

[53] S. P. Raman, M. Mahesh, R. V. Blasko, and E. K. Fishman, "CT scan parameters and radiation dose: practical advice for radiologists," J. Am. Coll. Radiol., vol. 10, no. 11, pp. 840–846, Nov. 2013.

[54] P. Rogalla, C. Kloeters, and P. A. Hein, "CT technology overview: 64-slice and beyond," Radiol. Clin. North Am., vol. 47, no. 1, pp. 1–11, Jan. 2009.

[55] B. C. V. Campbell et al., "CT perfusion improves diagnostic accuracy and confidence in acute ischaemic stroke," J. Neurol. Neurosurg. Psychiatry, vol. 84, no. 6, pp. 613–618, Jun. 2013.

[56] C. Bollwein et al., "Diagnostic accuracy of whole-brain CT perfusion in the detection of acute infratentorial infarctions," Neuroradiology, vol. 58, no. 11, pp. 1077–1085, Nov. 2016.

[57] I. H. Lee et al., "Accuracy of the detection of infratentorial stroke lesions using perfusion CT: an experimenter-blinded study," Neuroradiology, vol. 52, no. 12, pp. 1095–1100, Dec. 2010.

[58] K. Ogasawara, M. Sasaki, N. Tomitsuka, Y. Kubo, T. Inoue, and A. Ogawa, "Early Revascularization in a Patient With Perfusion Computed Tomography/Diffusion-Weighted Magnetic Resonance Imaging Mismatch Secondary to Acute Vertebral Artery Occlusion," Neurologia medico-chirurgica, vol. 45, no. 6. pp. 306–310, 2005, doi: 10.2176/nmc.45.306.

[59] O. Bill et al., "Focal Hypoperfusion in Acute Ischemic Stroke Perfusion CT: Clinical and Radiologic Predictors and Accuracy for Infarct Prediction," American Journal of Neuroradiology. 2019, doi: 10.3174/ajnr.a5984.

[60] M. Page et al., "Comparison of 4 cm Z-axis and 16 cm Z-axis multidetector CT perfusion," Eur. Radiol., vol. 20, no. 6, pp. 1508–1514, Jun. 2010.

[61] L.-P. Pallesen et al., "Diagnostic and Prognostic Impact of pc-ASPECTS Applied to Perfusion CT in the Basilar Artery International Cooperation Study," J. Neuroimaging, vol. 25, no. 3, pp. 384–389, May 2015.

[62] M. Wintermark, W. S. Smith, N. U. Ko, M. Quist, P. Schnyder, and W. P. Dillon, "Dynamic perfusion CT: optimizing the temporal resolution and contrast volume for calculation of perfusion CT parameters in stroke patients," AJNR Am. J. Neuroradiol., vol. 25, no. 5, pp. 720–729, May 2004.

[63] S. W. Youn, J. H. Kim, Y.-C. Weon, S. H. Kim, M.-K. Han, and H.-J. Bae, "Perfusion CT of the brain using 40-mm-wide detector and toggling table technique for initial imaging of acute stroke," AJR Am. J. Roentgenol., vol. 191, no. 3, pp. W120–6, Sep. 2008.

[64] M. P. Fabritius et al., "Incremental Value of Computed Tomography Perfusion for Final Infarct Prediction in Acute Ischemic Cerebellar Stroke," J. Am. Heart Assoc., vol. 8, no. 21, p. e013069, Nov. 2019.

[65] M. P. Fabritius et al., "Early Imaging Prediction of Malignant Cerebellar Edema Development in Acute Ischemic Stroke," Stroke, vol. 48, no. 9, pp. 2597–2600, Sep. 2017.

[66] K. W. Muir, A. Buchan, R. von Kummer, J. Rother, and J.-C. Baron, "Imaging of acute stroke," Lancet Neurol., vol. 5, no. 9, pp. 755–768, Sep. 2006.

[67] J. C. Kattah, A. V. Talkad, D. Z. Wang, Y.-H. Hsieh, and D. E. Newman-Toker, "HINTS to diagnose stroke in the acute vestibular syndrome: three-step bedside oculomotor examination more sensitive than early MRI diffusion-weighted imaging," Stroke, vol. 40, no. 11, pp. 3504–3510, Nov. 2009.

[68] C. Oppenheim et al., "False-negative diffusion-weighted MR findings in acute ischemic stroke," AJNR Am. J. Neuroradiol., vol. 21, no. 8, pp. 1434–1440, Sep. 2000.

[69] J. A. Chalela et al., "Magnetic resonance imaging and computed tomography in emergency assessment of patients with suspected acute stroke: a prospective comparison," Lancet, vol. 369, no. 9558, pp. 293–298, Jan. 2007.

[70] J.-H. Choi et al., "Early MRI-negative posterior circulation stroke presenting as acute dizziness," J. Neurol., vol. 265, no. 12, pp. 2993–3000, Dec. 2018.

[71] W. Schonewille, C. Wijman, and P. Michel, "Treatment and Clinical Outcome in Patients With Basilar Artery Occlusion," Stroke, vol. 37, no. 9. pp. 2206–2206, 2006, doi: 10.1161/01.str.0000237127.84408.c0.

[72] W. J. Schonewille et al., "Treatment and outcomes of acute basilar artery occlusion in the Basilar Artery International Cooperation Study (BASICS): a prospective registry study," Lancet Neurol., vol. 8, no. 8, pp. 724–730, Aug. 2009.

[73] J. Ravindren, M. Aguilar Pérez, V. Hellstern, P. Bhogal, H. Bäzner, and H. Henkes, "Predictors of Outcome After Endovascular Thrombectomy in Acute Basilar Artery Occlusion and the 6hr Time Window to Recanalization," Front. Neurol., vol. 10, p. 923, Sep. 2019.

[74] V. Puetz et al., "Extent of Hypoattenuation on CT Angiography Source Images in Basilar Artery Occlusion," Stroke, vol. 42, no. 12. pp. 3454–3459, 2011, doi: 10.1161/strokeaha.111.622175.

[75] F. Alemseged et al., "Cerebral blood volume lesion extent predicts functional outcome in patients with vertebral and basilar artery occlusion," Int. J. Stroke, vol. 14, no. 5, pp. 540–547, Jul. 2019.

[76] J. M. Biesbroek et al., "Diagnostic accuracy of CT perfusion imaging for detecting acute ischemic stroke: a systematic review and meta-analysis," Cerebrovasc. Dis., vol. 35, no. 6, pp. 493–501, May 2013.

[77] D. Y. Hwang, G. S. Silva, K. L. Furie, and D. M. Greer, "Comparative sensitivity of computed tomography vs. magnetic resonance imaging for detecting acute posterior fossa infarct," J. Emerg. Med., vol. 42, no. 5, pp. 559–565, May 2012.

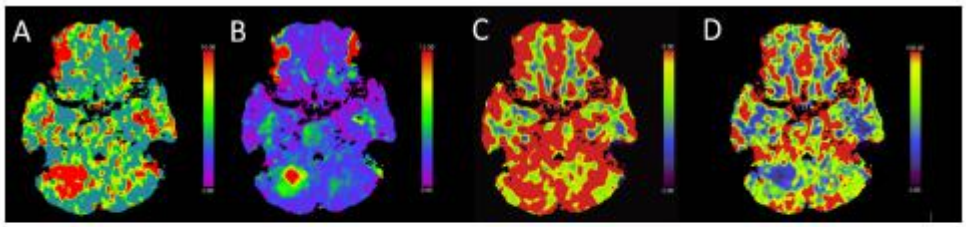

Figure-1A

Perfusion maps from an acute posterior circulation stroke causing right cerebellar infarction at 1 hour and 23 minutes after symptom onset. Thrombolysis was not given due to a National Institute of Health stroke score (NIHSS) of 0. Maps are from the Siemens syngo.CT Neuro perfusion package which include; (A) MTT, (B) Tmax, (C) CBV and (D) CBF. Images demonstrate an acute right cerebellar perfusion lesion with involvement of the superior cerebellar artery (SCA) vascular territory. No vessel occlusion was visualised on CT angiography. The perfusion lesion is most prominent on the (A) MTT and (B) Tmax and (D) CBF maps.

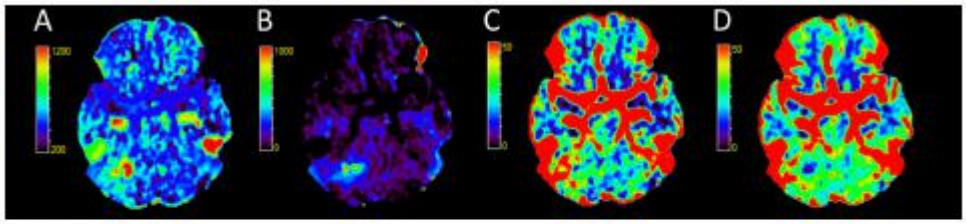

Figure-1B

Perfusion maps from the same acute posterior circulation stroke seen in Figure-1. Map outputs are from the MiStar neuro perfusion package which include; (A) MTT, (B) DT, (C) CBV and (D) CBF. Images demonstrate an acute right cerebellar lesion most evident on the (A) Tmax, (B) DT and (D) CBF maps. Similar to the Siemens syngo.CT Neuro perfusion package, the acute lesion is not well visualised on the CBV map. There is a notable difference in the volume of the perfusion lesion seen across the packages. This reflects the different algorithms employed by the two software proprietors in determination of the perfusion maps.

625

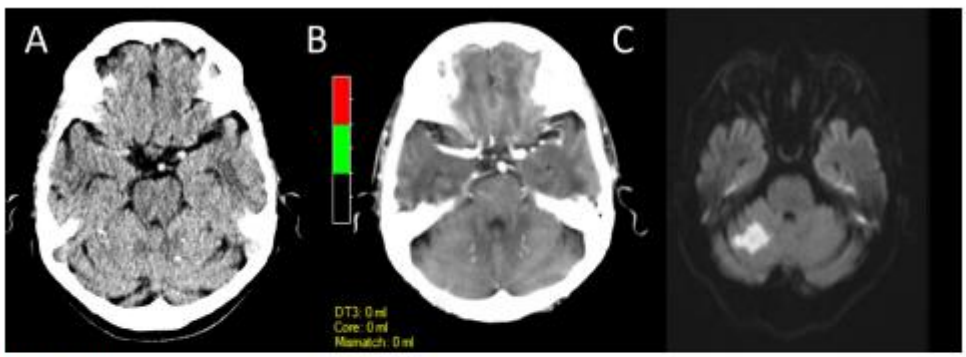

Figure-1C

Evolution of the acute posterior circulation stroke demonstrated in Figure-1 and Figure-2. (A) Initial non-contrast CT at 1 hour and 23 minutes after symptom onset demonstrates no acute change. (B) Initial automated core-penumbra map from the MiStar neuro perfusion package using the conventional thresholds for core and penumbra of CBV <30% and DT>3 seconds demonstrates no detectable perfusion lesion (although this may also relate to the relatively small size of the lesion as the software has a minimum volume criteria for core/penumbra to try to reduce false core/penumbra from 'noise). (C) Progress diffusion weighted magnetic resonance imaging at 20h and 30 minutes after onset of symptoms demonstrating an established left cerebellar infarct.

626

627

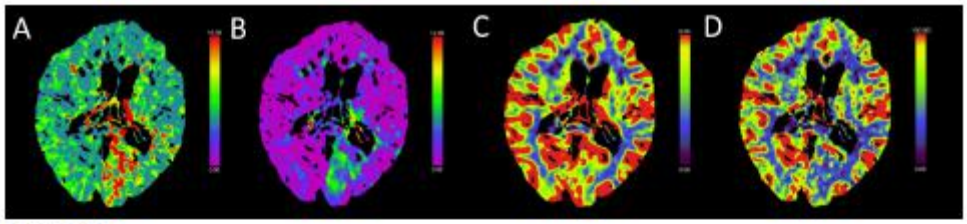

Figure-2A

Perfusion maps from an acute posterior circulation stroke causing left posterior cerebral artery infarction at 7 hours and 15 minutes after last known well time. Maps are from the Siemens syngo.CT Neuro perfusion package which include; (A) MTT, (B) Tmax, (C) CBV and (D) CBF. Images demonstrate an acute left occipital perfusion lesion involving the posterior cerebral artery vascular territory. The vessel occlusion was not seen on CT angiography. Changes are most prominent on the (A) MTT and (B) Tmax and (D) CBF maps.

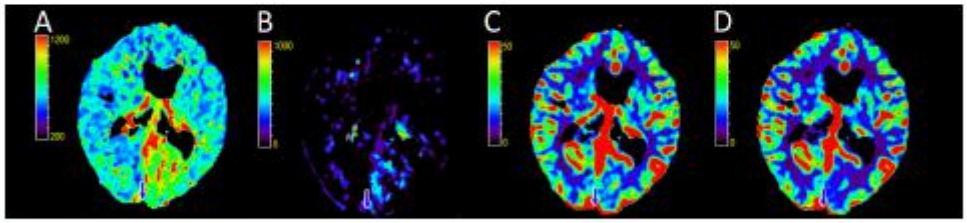

Figure-2B

Perfusion maps from the same acute posterior circulation stroke seen in Figure-1. Map outputs are from the MiStar neuro perfusion package which include; (A) MTT, (B) DT, (C) CBV and (D) CBF. Images demonstrate an acute left occipital lesion most evident on the (A) Tmax, (B) DT and (D) CBF maps. Similar to the Siemens syngo.CT Neuro perfusion package, the acute lesion is not well visualised on the CBV map. There is a notable difference in the volume of the perfusion lesion seen across the packages. This reflects the different algorithms employed by the two software proprietors in determination of the perfusion maps.

628

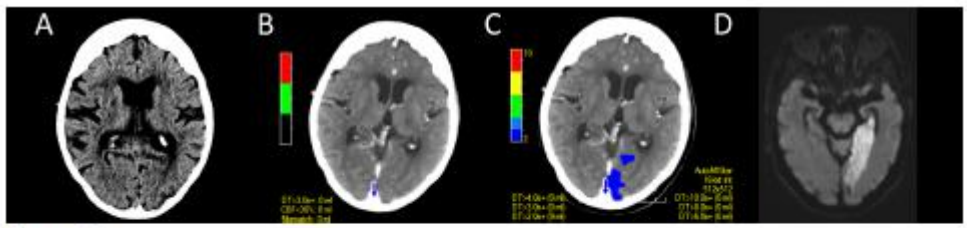

Figure-2C

Evolution of the acute posterior circulation stroke demonstrated in Figure-1 and Figure-2. (A) Initial non-contrast CT at 7 hours and 15 minutes after last known well time demonstrates no acute change. (B) Initial summary map from the MiStar neuro perfusion package using the conventional thresholds for core and penumbra of CBV <30% and DT>3 seconds does not demonstrate a detectable perfusion lesion. (C) Delay time map demonstrates a perfusion lesion at the threshold of DT>2 seconds (but below the DT 3 seconds threshold for 'penumbra'. (D) Progress diffusion weighted magnetic resonance imaging at 24h and 40 minutes after last known well time demonstrating an established right posterior cerebral artery infarct. Discordance with the automated map and similarity to the DT >2 lesion suggest conventional perfusion thresholds are not optimised for posterior circulation strokes. Both cases also highlight the need not to simply rely on the core/penumbra maps, but to look at all the perfusion maps.

629

630

631

632

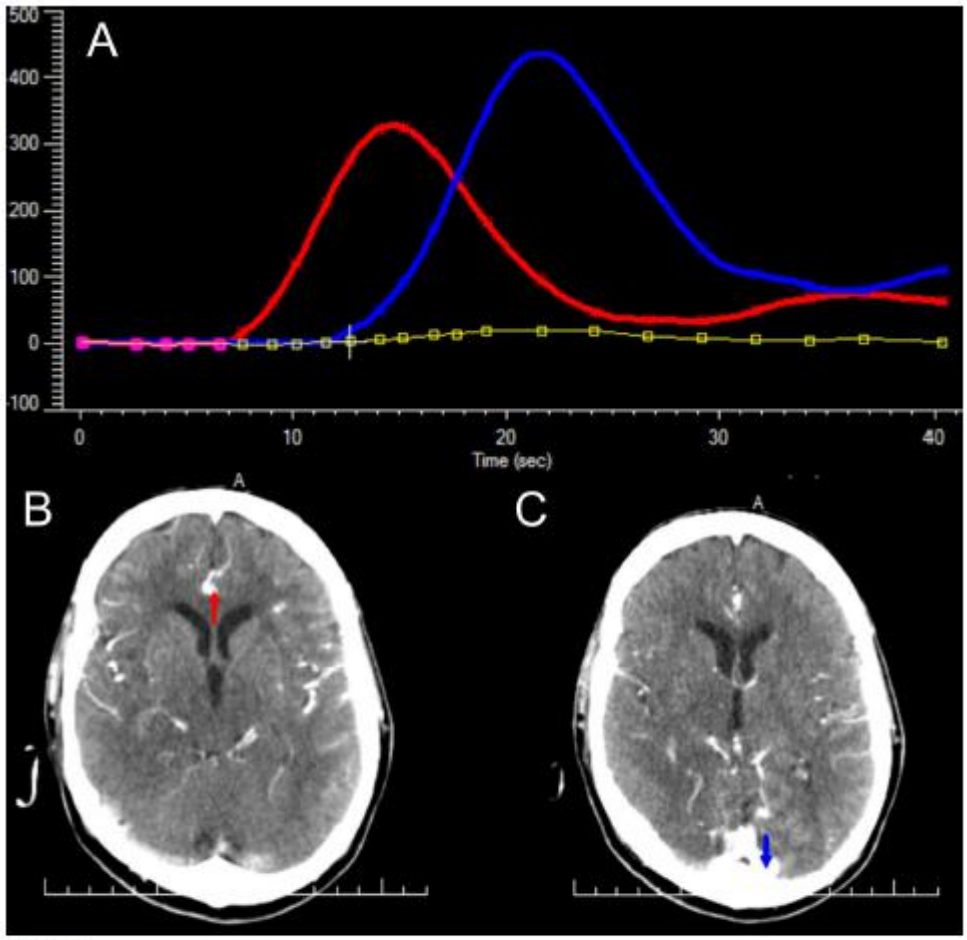

Figure 3

CTP parameters are derived from the measurement of the transit of iodinated contrast through the cerebral vessels and parenchyma. The arterial input function (AIF) and venous output function (VOF) underpin the mathematical calculation of these parameters. (A) A visual representation of the AIF (red line) and VOF (blue line) of an acute basilar artery occlusion 1 hour after stroke onset. Mistar neuroperfusion package automatically selects (B) an artery from the anterior circulation for calculation of the AIF and (C) a venous sinus for calculation of the VOF.

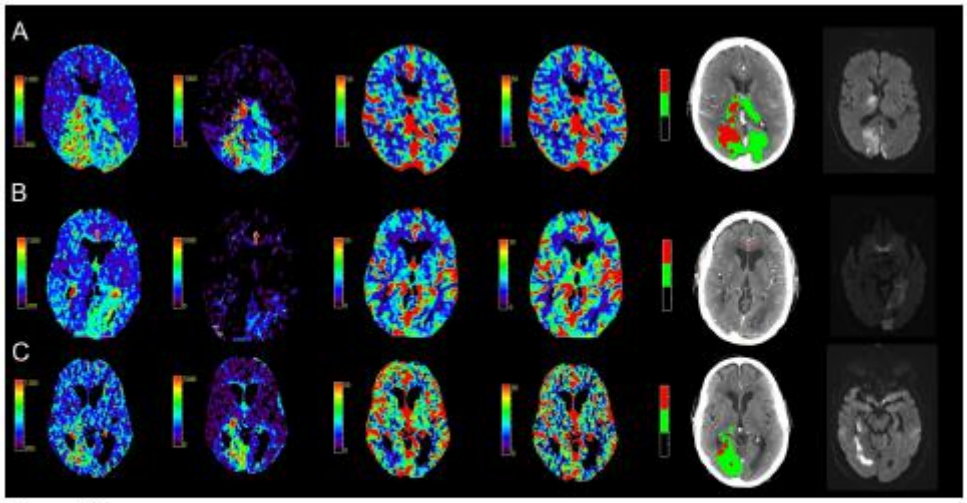

Figure-4A

A spectrum of PCS perfusion patterns involving the posterior cerebral artery territory (PCA). From left to right displayed imaging includes: mean transit time, delay time, cerebral blood volume, cerebral blood flow, automated core-penumbra map and 24 hour diffusion weighted MRI. Perfusion maps generated using MiStar neuroperfusion package. (A) Bilateral PCA stroke due to distal basilar artery occlusion. (B) Left PCA stroke due to a left P1 segment occlusion. (C) Right PCA territory infarction due to a right P1 segment occlusion.

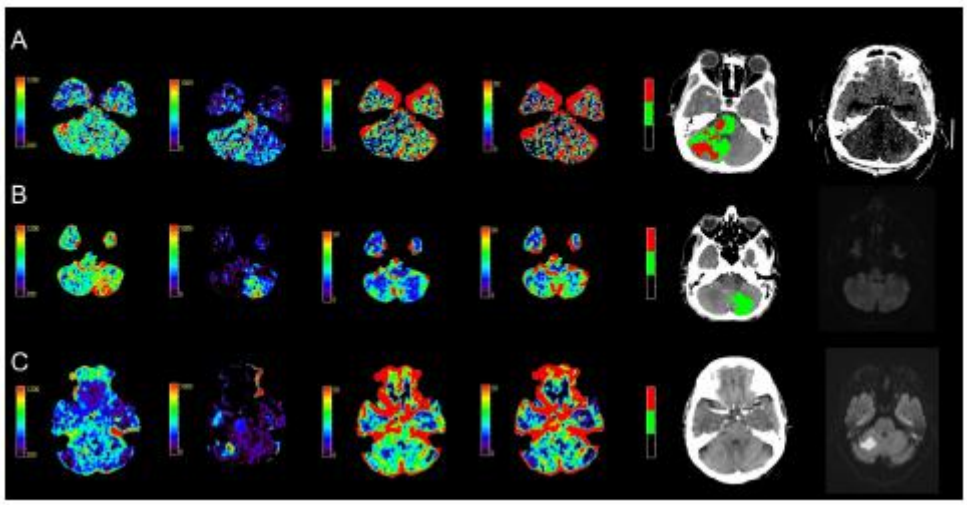

637 **Figure-4B**

PCS perfusion patterns involving the cerebellar hemispheres. From left to right displayed imaging includes: mean transit time, delay time, cerebral blood volume, cerebral blood flow, automated core-penumbra map and 24 hour imaging (diffusion weighted MRI or non-contrast CT brain). Perfusion maps generated using MiStar neuroperfusion package. (A) A mid basilar occlusion causing a significant brainstem and right cerebellar perfusion lesion. No visible occlusion on vessel imaging with a (B) left and (C) right posterior inferior cerebellar artery territory stroke.

638